

Evaluating Local Distribution Grid Capacity Under PV Energy Injection

Toussaint Tilado Guingane^{1,2,*}, Éric Korsaga², Sosthène Tassemedo²,
 Ousmane Sawadogo³, Raguilignaba Sam^{2,3}, Zacharie Koalaga²

¹Laboratoire de Sciences et Technologies (LaST), Université Thomas SANKARA, Ouagadougou, Burkina Faso

²Materials and Environment Laboratory, Université Joseph Ki ZERBO Ouagadougou, Burkina-Faso

³Université Nazi BONI, Bobo Dioulasso, Burkina-Faso

*Corresponding author: tilado88@yahoo.fr

Received November 01, 2024; Revised December 02, 2024; Accepted December 09, 2024

Abstract This paper assesses the capacity of a low-voltage distribution network to receive photovoltaic energy. A simulation is carried out in Matlab/Simulink, taking into account the elements representative of the photovoltaic system connected to the grid. The PV generator is simulated under nominal operating conditions. The analyses focus on the total harmonic distortion (THD) of the current and the grid voltage level. Data Analysing collection within the stability limits enabled us to identify a threshold for the penetration rate of 8 to 10% and a maximum penetration rate of around 47%. This is justified by the voltage drop and the unconditional nature of power flows at the limits of massive injections. Injections below the determined threshold have proved to be sources of pollution for the network, while massive injections change the direction of power flow.

Keywords: distribution grid, PV system, active power, reactive power, THD

Cite This Article: Toussaint Tilado Guingane, Éric Korsaga, Sosthène Tassemedo, Ousmane Sawadogo, Raguilignaba Sam, and Zacharie Koalaga, "Evaluating Local Distribution Grid Capacity Under PV Energy Injection." *American Journal of Energy Research*, vol. 12, no. 4 (2024): 70-76. doi: 10.12691/ajer-12-4-1.

1. Introduction

Photovoltaic energy is a promising alternative to fossil fuels, particularly in developing countries. Decentralised production offers new applications, such as supplying low-voltage distribution. There are an increasing number of self-consumption production units, with small capacities connected to the Low Voltage (LV) distribution network and solar farms connected directly to the Medium Voltage (MV) network. This solution bridges the gap between supply and demand.

However, connecting PV systems to an electricity grid is fraught with technical problems and unpredictable consequences for both the grid and the PV installation.

Previous studies [1,2,3,4] have shown the impact of PV penetration on the power factor of the LV network [4,5,6,7].

This work proposes to evaluate the integration capacity of PV solar energy in the LV distribution network using Matlab simulations. Low-voltage distribution offers few possibilities for forecasting production, and the intermittency of PV production makes it difficult to control power flows, and therefore voltage and frequency stability [7,8,9,10,11,12]. It is therefore necessary to determine the maximum injection rate that will not affect the voltage level or frequency of the distribution network.

2. Topology of the Adopted Grid Tied PV System

Figure 1 shows the topology of the grid tied PV system adopted for the purpose of the study. It includes a PV generator, a boost converter, a voltage source converter (VSC), an LC-type filter, a transformer and a grid utility [3,12,13].

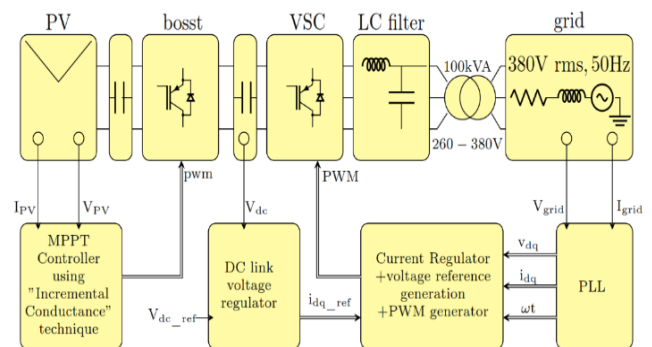


Figure 1. Topology of the grid tied PV system

2.1. PV Generator

The panel we are using as a reference is the SunPower

A300 produced and marketed by SunPower Corporation. It is certified to IEC 61215 Ed.2, IEC 61730 (SCII). The parameters of one cell in this panel are listed in Table 1. Each A300 panel consists of $N_s = 96$ back-contact monocrystalline cells, connected in series with a nominal size of 125 mm x 125 mm and a thickness of $250\mu\text{m} \pm 30\mu\text{m}$.

2.2. Boost Converter

A 5kHz DC-DC boost converter is used to increase the PV generator natural voltage (273V at the maximum power). The switching duty cycle of the converter is optimized by an MPPT controller using the “Incremental Conductance” technique [13,14,15,16]. the Boost c model

is given in the Figure 2.

2.3. Inverter

We consider a three-level double voltage converter bridge (VSC). This is a reversible converter whose switches each consist of an IGBT in parallel with a free-wheeling diode. They operate like control valves. In this configuration, the role of the filter, consisting at least of inductance, is twofold. Firstly, it attenuates current variations during switching and, secondly, it filters higher-order harmonics. There are six phases in an operating cycle, and the states of the switches are shown in Table 1 below. [17]

The Figure 3 shows the inverter in its operating chain.

Table 1. Operating states of a three-level VSC

Phase	s_{1k}	s_{2k}	s_{3k}	s_{4k}	i_{0k}	v_{0k}	path of i_{0k}
1	duct	duct	blocked	blocked	> 0	$\frac{v_{dc}}{2}$	s_{1k}, s_{2k}
2	duct	duct	blocked	blocked	< 0	$\frac{v_{dc}}{2}$	d_{1k}, d_{2k}
3	blocked	blocked	duct	duct	> 0	$-\frac{v_{dc}}{2}$	d_{3k}, d_{4k}
4	blocked	blocked	duct	duct	< 0	$-\frac{v_{dc}}{2}$	s_{3k}, s_{4k}
5	blocked	duct	duct	blocked	> 0	0	s_{2k}, D_{Zk}
6	blocked	duct	duct	blocked	< 0	0	s_{3k}, D_{Yk}

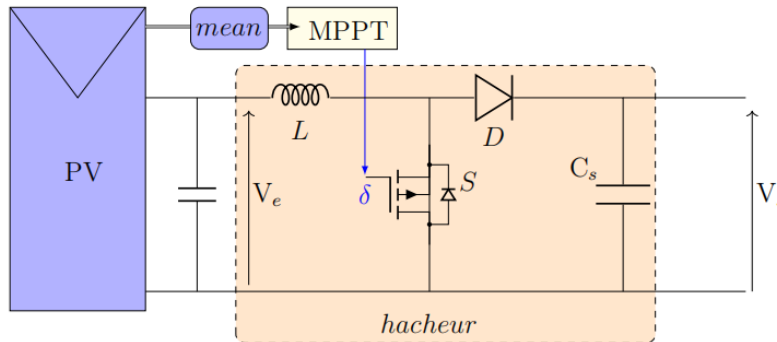


Figure 2. Boost controller in the operating chain

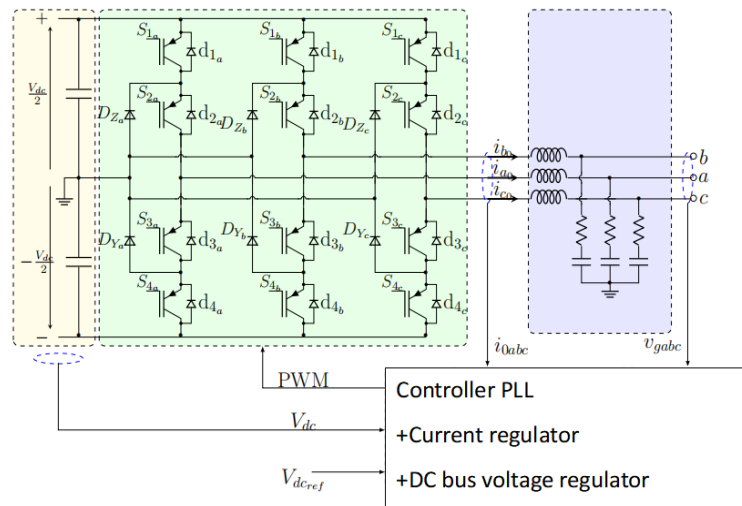


Figure 3. Inverter in its operating chain

2.4. VSC and the LC-type Filter

A 1450-Hz, three phases and three levels Neutral Point Clamp (NPC) inverter is used to convert the 500V DC-link voltage to 260V AC with unity power factor. The command of the inverter a decouple dq frame control technique [8]. It includes a DC-link voltage regulator, a current regulator with feedforward-an internal control loop witch regulate active and reactive components of the grid current.

An LC- type filter is designed to filter harmonics produced by the VSC by the means of a capacitor and an inductor. [15]

2.5. Transformer and Utility Grid

A 100kVA 260V/380V three phase coupling transformer is used to tie the system to the utility grid witch is a balanced three phase voltage source with an internal L-R impedance.

The internal phase to phase voltage of the grid in rms is 380V under a 50Hz nominal frequency.

2.6. Algorithm

Many methods exist in the literature, but in our work we have chosen the IncCond method because of its high efficiency in optimising the maximum power. Solar panel operation is governed by a power-voltage (P-V) curve, which has a single maximum power point (MPP). The IncCond algorithm relies on a comparison between instantaneous conductance (I/V) (I/V) and incremental conductance ($\Delta I/\Delta V$) ($\Delta I/\Delta V$) to determine whether the system is before, after or at the MPP on the P-V curve.

How the algorithm works:

- 1) Measurement of parameters: The algorithm measures the instantaneous values of voltage V and current I.
- 2) Calculating variations: It calculates the incremental variations in voltage (ΔV) and current (ΔI).
- 3) Analysis of conditions:
 - If $(\Delta I/\Delta V + I/V) = 0$ ($\Delta I/\Delta V + I/V) = 0$, the system is at MPP.

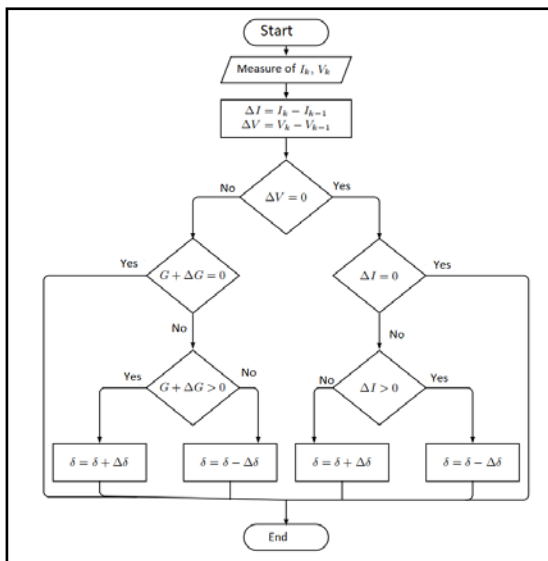


Figure 4. IncCond flowchart method

- If $(\Delta I/\Delta V + I/V) > 0$ ($\Delta I/\Delta V + I/V) > 0$, the system is before MPP, and the voltage must be increased.

- If $(\Delta I/\Delta V + I/V) < 0$ ($\Delta I/\Delta V + I/V) < 0$, the system is after MPP, and the voltage should be decreased.

4) Voltage adjustment: The algorithm adjusts the inverter input voltage (boost or buck) to get closer to the MPP.

Repetition: These steps are repeated in a loop to monitor variations in operating conditions in real time.

Its scheme is shown in Figure 4. [18,19]

3. Study Approach

We stabilize the production of the PV generator by maintaining nominal operating conditions ($G=1000W/m^2$ and $T=25^\circ C$). Analysis and their conclusion are relative to IEEE 1547 standards [3] ($THD \leq 5\%$ and $\Delta V/V \leq 5\%$). Figure 5 shows the evolution of the power produced by the PV generator with the number of array N_p for different short-circuit power. The power grows linearly with N_p and can be indexed over N_p .

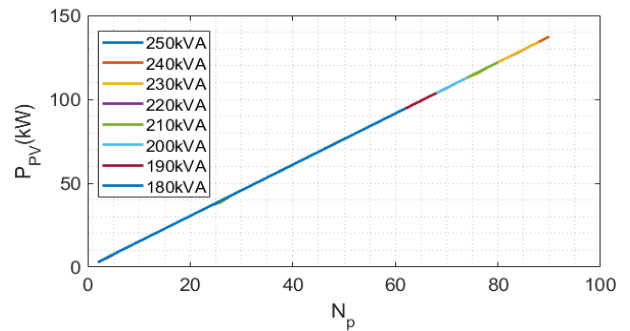


Figure 5. Evolution of the PV generator power with N_p

Grid voltage stability collapse during relatively massive feeding suggest a maximum injection rate. Fig.6 show a phase signal aspect of the grid voltage during a massive injection ($N_p=100$) with 250kVA short-circuit power.

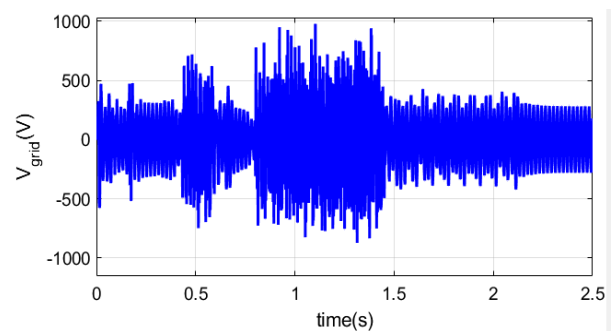


Figure 6. Evolution of the grid voltage signal during excessive feeding

4. Results and Discussion

4.1. Mass Injection

The degradation of the voltage profile associated with a massive injection of photovoltaic energy into the grid is directly influenced by the short-circuit power of the grid, which determines its capacity to absorb power fluctuations. A short-circuit power of 250 kVA has been considered to

assess these limits, and the simulations have been carried out taking into account progressive injection until significant degradation of the voltage plane occurs.

Figure 7 shows the voltage evolution on one network phase for a massive injection corresponding to $N_p=100$ photovoltaic producers. These tests have shown that increasing PV production above certain thresholds leads to a significant deterioration in power quality parameters, in particular:

- Voltage variations: Grid voltage must comply with the limits defined by IEEE standards, i.e. a maximum variation of $\pm 5\%$. Beyond this limit, electrical equipment connected to the network may malfunction.

- Total harmonic distortion (THD): THD, which measures voltage quality, must remain below 5%. Poorly controlled photovoltaic production can introduce additional harmonics, impacting the quality of the energy delivered.

These results highlight the need to limit the injection capacity of each PV unit or to improve network management in order to maintain performance within the acceptable limits of IEEE standards. In this context, solutions such as integrating advanced control systems (voltage regulation, injection of compensating harmonics) or increasing the network's short-circuit power (increasing the capacity of transformers or lines) could be considered.

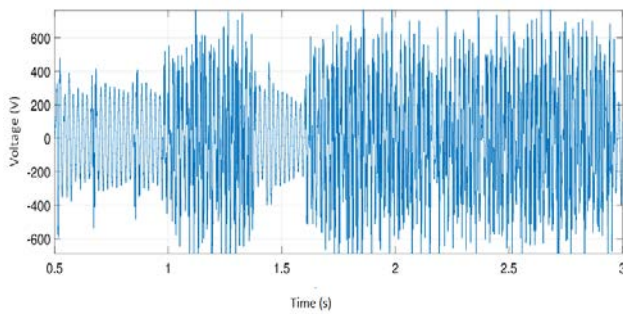


Figure 7. Voltage on a network phase for massive injection

4.2. Feeding Efficiency and THD

The topology adopted in the system imposes critical power thresholds to guarantee an efficient power supply and maintain optimum operation of the transformer. These thresholds, linked to the power of the connected photovoltaic generators (N_p) and the short-circuit power of the grid, directly influence the overall performance of the system.

Figure 8 shows the evolution of supply efficiency as a function of different short-circuit powers. It shows that a minimum value of $N_p=18$ is required to achieve an efficient power supply. Below this threshold, losses in the network increase considerably, making the system less efficient. This threshold is an essential feature of the chosen topology, as it ensures compatibility between the capacity of the generators and the requirements of the network.

At the same time, this topology also imposes limitations in terms of power quality, specifically concerning total harmonic distortion (THD). N_p values below 18 lead to a significant increase in THD, causing harmonic pollution of the network, which can compromise the stability of the electrical equipment connected. Figure 9 clearly shows that for a given short-circuit power, the minimum value of N_p required to maintain a tolerable THD (below 5%, in

accordance with IEEE standards) is also approximately $N_p=18$.

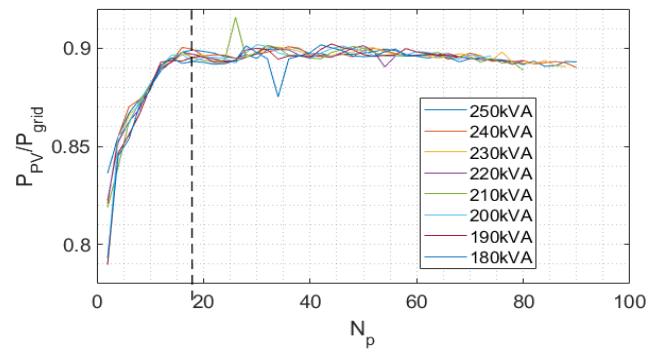


Figure 8. Evolution of the feeding yield for different short-circuit power

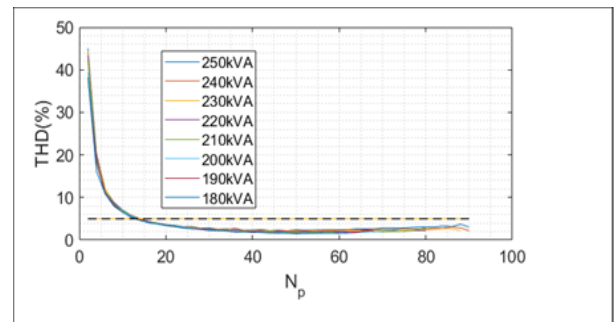


Figure 9. Evolution of the THD for different short-circuit power

These results reveal two critical aspects of the topology adopted:

- Energy efficiency: Feed efficiency is highly dependent on the number of photovoltaic generators connected and their ability to inject sufficient power to overcome losses.

- Power quality: Harmonic management becomes a major challenge when production is insufficient, as high THD values can disturb sensitive equipment and reduce network reliability.

To guarantee optimal operation, the number of photovoltaic generators needs to be kept above the critical threshold of $N_p=18$. Appropriate planning and control measures such as adding harmonic filters or improving the short-circuit power of the grid (by reinforcing equipment or integrating advanced technologies) can be considered to improve the overall performance of the system and limit the negative impact on power quality.

4.3. Grid Voltage Rms Evolution

Figure 10 shows the evolution of the RMS network voltage as a function of different short-circuit powers. This shows the non-linear behaviour of the voltage, which goes through a phase of increase before reaching a maximum, followed by a decrease. This phenomenon reflects the interaction between the active power injected by the photovoltaic sources and the reception capacity of the grid, which is strongly influenced by the reactive power parameters.

Initially, the injection of active power by the PV sources leads to a rise in voltage at the connection point. This behaviour is due to the predominance of active power in the overall power factor, which reduces losses and

stabilises voltage levels. However, as active power continues to increase and exceeds the network's proportional capacity to manage reactive power (linked to short-circuit power and infrastructure characteristics), the network enters a phase of imbalance.

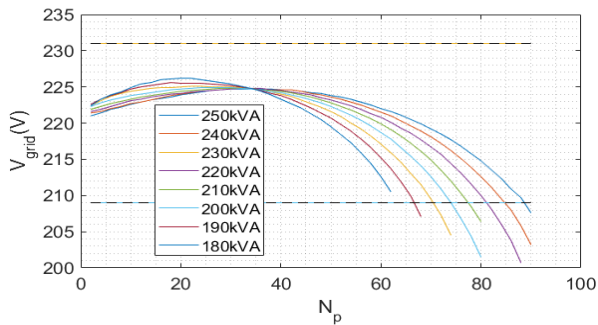


Figure 10. grid voltage rms evolution for different short-circuit power

Beyond this critical point, compensation for the reactive power imbalance becomes predominant, leading to a drop in effective voltage. This drop can reach critical levels, crossing the lower limit of 209 V, indicating an inability of the network to maintain power quality standards (according to IEEE standards). This phenomenon can lead to problems for sensitive equipment connected to the network, such as variations in performance or power cuts.

4.4. Feeding Rate Evolution

The feeding rate evolution is linear. It increases with the number of array N_p . Figure 11 show the evolution of the feeding rate for different short-circuit power.

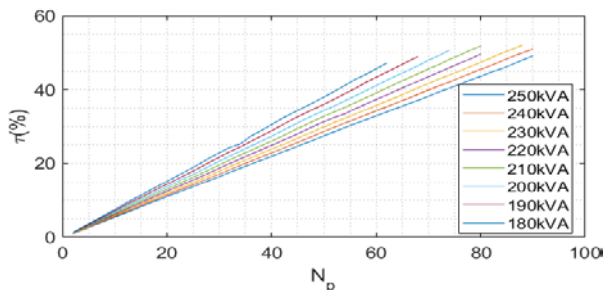


Figure 11. feeding rate evolution for different short-circuit power

4.4. Threshold and Maximum Rate

By comparing the various constraints imposed by Total Harmonic Distortion (THD) limits and voltage variations, it is possible to identify the critical thresholds for injecting power into the network. These limits make it possible to define the optimum operational ranges for guaranteeing power quality and network stability.

The analyses show that:

- The lower limit of the injection rate, between 8% and 10%, corresponds to the minimum required to maintain acceptable total harmonic distortion (THD) (according to IEEE standards, $THD < 5\%$). Below this threshold, low injection levels can aggravate harmonic pollution and compromise the performance of connected equipment.
- The upper limit, around 47%, is determined by the voltage drop. Above this threshold, the voltage at the connection point drops significantly, exceeding the

permissible tolerance standards ($\pm 5\%$ of the nominal voltage). This phenomenon results from overloading the network with active power, which leads to instability in reactive power management.

Figure 12 illustrates these limit rates as a function of injection conditions and network parameters. This visualization highlights the safe injection ranges and the risk zones where significant degradation can occur.

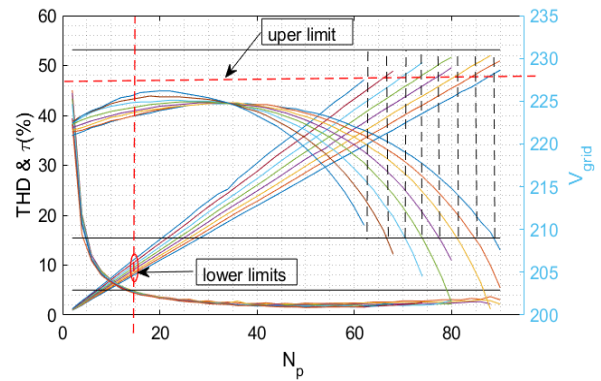


Figure 12. Limit rates determination

4.5. Grid Influences on the PV System

The evaluation of certain key parameters of the photovoltaic (PV) generator under a massive injection condition ($N_p = 100$) and a short-circuit power of 250 kVA highlights critical behaviours of the system. In particular, Figure 13 illustrates the evolution of the DC bus voltage during injection.

It can be seen that:

- The DC bus voltage no longer manages to follow the set value: This instability indicates an inability of the regulator to maintain control over the bus voltage, probably due to excess power injected into the system or an overload of the PV generator components.
- A significant voltage overshoot is observed, reaching a peak equivalent to 6 times the nominal capacity of the generator. This phenomenon reflects a mismatch between the energy produced by the PV modules and the absorption or regulation capacity of the system, which can lead to significant risks for the stability of the power grid and the integrity of the equipment.

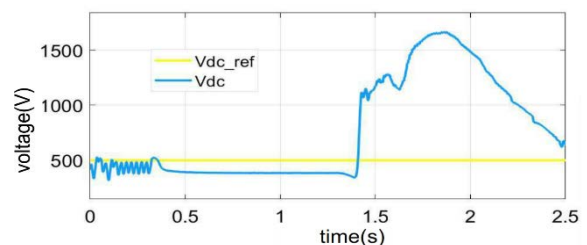


Figure 13. Evolution of the DC-link voltage compare to the reference during massive injection

Figure 14 shows how the voltage across the photovoltaic array (V_{PV}) changes over time. Although irradiation and temperature are kept constant, the voltage undergoes significant oscillations. This fluctuating behaviour is particularly noticeable, as the voltage even reaches negative values at certain times.

- Voltage oscillations: The appearance of these oscillations indicates instability in the behaviour of the PV generator, generally caused by an imbalance between the generator's energy production and the system's capacity to absorb this energy. These fluctuations may be due to a complex interaction between the system's electronic components, such as converters and power regulators.

- Negative voltage values: The fact that the voltage at the generator terminals becomes negative suggests a phenomenon of 'receiver behaviour' of the photovoltaic generator, where it starts to absorb energy instead of producing it. This can occur when too much energy is injected into the grid to be properly managed by the conversion devices, or when the system is overloaded. generator exhibits receptor behavior under massive injection.

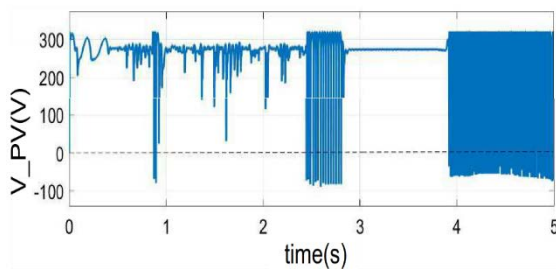


Figure 14. Evolution of the PV generator voltage during massive injection

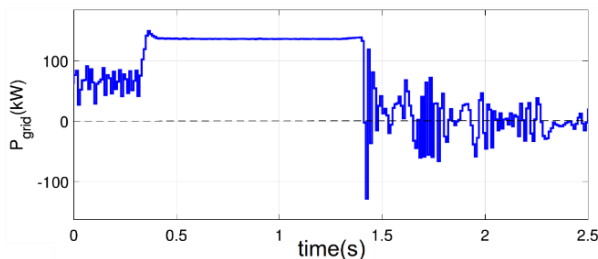


Figure 15. Evolution of grid power under massive feeding

Figure 15 shows the evolution of the power injected into the network as a function of time. The observation reveals an inconsistency between the profile of the power injected and the irradiation profile initially defined (with an irradiation of 1000 W/m^2). The curve shows a cancellation of the injected power, followed by negative values, indicating a reversal of the power flow.

- Reversal of power flow: This reversal, where the power that would normally flow from the photovoltaic (PV) array to the grid is reversed, is a critical phenomenon. It is mainly caused by the reversible nature of the Voltage Source Converter (VSC) used in grid-connected photovoltaic systems. The VSC not only transforms power from the PV generator into power fed into the grid, it can also work in the opposite direction, absorbing energy from the grid to feed the PV generator, particularly during overload conditions.

- Reversible nature of the VSC: The VSC is designed to be flexible in managing active and reactive power. During a massive injection of energy, if the grid's capacity to absorb this energy is limited or if demand exceeds supply, the system can lead to a 'reverse power flow' phenomenon, where the excess energy starts to flow in the

opposite direction, from the grid to the PV generator. This phenomenon can be accentuated in network or converter configurations that are not sufficiently adapted to manage such situations, resulting in abnormal fluctuations in the power injected.

5. Conclusion

In this article, several scenarios were simulated to assess the ability of a low-voltage (LV) network to integrate the injection of photovoltaic energy. The photovoltaic generator was simulated under nominal operating conditions, providing a detailed analysis of the behaviour of the network under different solar energy penetration rates. The data collected enabled specific penetration thresholds to be defined, revealing a minimum penetration rate of 8 to 10% beyond which disturbances begin to appear, and a maximum rate of around 47%, where notable effects such as voltage drop and power flow reversal become critical.

Injecting energy below these thresholds is problematic for the grid, causing excessive harmonic pollution and instability of electrical parameters. On the other hand, massive injections above the 47% threshold lead to a significant change in the direction of energy flow, pushing electricity from the grid towards the photovoltaic array due to the reversible nature of the voltage source converter (VSC). This reverses the energy flow, which can lead to frequency and voltage imbalances, threatening grid stability.

To compensate for these voltage variations and improve network stability, solutions such as LDCs (Line Drop Compensators) have been identified as being particularly effective. These devices make it possible to compensate for voltage drops by adjusting the transformer output in stages, thereby ensuring finer, more stable regulation of the voltage in the network. Adaptive management of the power injected, combined with energy storage devices and dynamic protection mechanisms, seems to be essential to avoid the risks associated with overproduction or uncontrolled injection of photovoltaic energy into the grid.

References

- [1] Yuanzhao Li et al., "Distributed PV Carrying Capacity Prediction and Assessment for Differentiated Scenarios Based on CNN-GRU Deep Learning," *Frontiers in Energy Research*, 2023. ISSN: 2296-598X.
- [2] Xiaoling Zhang et al., "Comprehensive Evaluation of Distributed PV Grid-Connected Based on Combined Weighting Weights and TOPSIS-RSR Method," *Energy Engineering*, 2024.
- [3] A. Smith et al., "Impact of High PV Penetration on Local Distribution Grid Capacity and Voltage Stability," *Renewable Energy*, 2023. ISSN: 0960-1481.
- [4] B. Johnson et al., "Optimization of Local Distribution Network Operations under High PV Injection Scenarios," *Applied Energy*, 2022. ISSN: 0306-2619.
- [5] R. Chen et al., "Evaluating the Resilience of Distribution Networks with High Penetration of Distributed PV," *Energy Reports*, 2023. ISSN: 2352-4847.
- [6] L. Wang et al., "Advanced Methods for Local Grid Stability Assessment under Increasing Solar PV Penetration," *Journal of Power Systems Engineering*, 2022. ISSN: 2227-9245.
- [7] IRENA (2021), Renewable capacity statistics 2021 International Renewable Energy Agency.

- [8] T. T. Guingane et al, impact de la pénétration du photovoltaïque sur le réseau électrique, American Journal of Innovative Research and Applied Sciences. ISSN 2429-5396.
- [9] T. T Guingane et al, Photovoltaic System Connected to the Grid without Battery Storage as a Solution to Electricity Problems in Burkina Faso. International Journal of Engineering Research. 2017, Volume No.6, Issue No, ISSN:2319-6890.
- [10] Jean-Marcel Rax, physique de la conversion d'énergie, EDP Sciences, 2015, ISBN: 978-2-7598-0792-5, p270-301.
- [11] Antonio Luque and Steven Hegedus, Handbook of Photovoltaic Science and Engineering, John Wiley & Sons, 2003, ISBN 0-471-49196-9, p-80.
- [12] Thomas Mambrini. Caractérisation de panneaux solaires photovoltaïques en conditions réelles d'implantation et en fonction des différentes technologies. Météorologie. Université Paris Sud - Paris XI, 2014. Français. NNT: 2014PA112380. tel-01164783.
- [13] L. Stoyanov. Etude de différentes structures de systèmes hybrides à sources d'énergie renouvelable. PhD thesis, Université de Corse Pasquale Paoli, 28 octobre 2011.
- [14] R. Teodorescu and al, Grid Converters for Photovoltaic and Wind Power Systems Grid Synchronization in Three Phase t. 2011.
- [15] électriques. Electronique. Université de Poitiers ; École nationale d'ingénieurs de Tunis (Tunisie), 2021. Français. NNT: 2021POIT2262. tel-03343654.
- [16] Fang Lin and Luo Hong Ye, advanced DC/AC inverters: applications in renewable energy, Taylor & Francis Group, ISBN 13: 978-1-4665-1138-5, 2013.
- [17] T. Esum, P.L. Chapman, Comparison of photovoltaic array maximum power point tracking techniques, IEEE Trans. Energy Conver. 22 (2) 439-449, 2007.
- [18] Hanen Abbes et al, Etude comparative de cinq algorithmes de commande MPPT pour un système photovoltaïque, International Journal of Control, Energy and Electrical Engineering (CEEE), ISSN 2356-5608.
- [19] Nedjma Aouchiche. Conception d'une commande MPPT optimale à base d'intelligence artificielle d'un système photovoltaïque.. Autre. Université Bourgogne Franche-Comté, 2020.



© The Author(s) 2024. This article is an open access article distributed under the terms and conditions of the Creative Commons Attribution (CC BY) license (<http://creativecommons.org/licenses/by/4.0/>).